Molecular aggregates, dendrimers, and motors

Augulis, Ramunas

Publication date:
2008

Citation for published version (APA):
Augulis, R. (2008). *Molecular aggregates, dendrimers, and motors: optical dynamics and control.* Groningen: s.n.

Chapter 5

Relaxation of Excitons in Tubular Molecular Aggregates at Low Temperatures: Time-resolved Transient Absorption Dynamics[*]

ABSTRACT

The fundamental aspects of exciton dynamics in double-wall cylindrical aggregates of cyanine dyes are studied by means of frequency resolved femtosecond pump-probe spectroscopy. The collective excitations of the aggregates, resulting from intermolecular dipole-dipole interactions show, as one of their characteristic properties, localization of the lowest lying exciton states. As a result, the experimentally observed outer-to-inner tubule excitonic energy transfer dynamics and the internal energy relaxation at low temperatures reveal a non-equilibrium population of the excitonic subsystem. In addition, the analysis of the measured dynamics reveals a very fast picosecond timescale energy relaxation to the optically active energy states.

I. INTRODUCTION

Molecular aggregates of organic dyes are attention-grabbing supra-molecular structures with a unique linear and non-linear optical response as well as intriguing optical energy transport properties. They are of fundamental interest as model materials to study the nature of excitons in systems of reduced dimensionality. Self-assembled cyanine dye J-aggregates were first reported by Jelley [1] and Scheibe [2] in the mid-thirties of the last century. The characteristic feature of J-aggregates is a narrow excitonic absorption band which is red-shifted with respect to the absorption of monomers and originates from an important interaction between the transition dipoles of neighbouring chromophores. During the last decades J-aggregates were studied extensively [3, 4]. Their large absorption cross-section in certain spectral region led to applications in the photographic industry [5] and potential use in the field of opto-electronics [3, 6]. Since natural light harvesting antennas are based on molecular aggregates, synthetic J-aggregates are considered as prospective building blocks for artificial light harvesting systems [7-9].

Self-aggregation of various cyanine and porphyrin dyes leads to a large variety of morphologies of J-aggregates ranging form quasi-linear molecular chains [3, 4] and

---

[*] This chapter is based on: R. Augulis, A. Pugžlys, and P. H. M. van Loosdrecht, *Phys. Stat. Sol. (c)* **3**, 3400 (2006).

molecular rings [9, 10] to single-, double- and multi-wall tubules [7, 11-13]. In this chapter we focus on the exciton dynamics of double-wall tubular aggregates of the 3,3'-bis(3-sulfopropyl)-5,5',6,6'-tetrachloro-1,1'-dioctylbenzimidacarbocyanine dye (C8S3) (chemical structure is shown in Fig. 1). Cryo-TEM experiments reveal a double wall tubular morphology of C8S3 aggregates with diameters of (15.6 ± 0.5) and (10.8 ± 0.5) nm for the outer and inner tubules respectively [12]. The collective excitations of the aggregates, resulting from the dipole-dipole interactions between the transition dipole moments of neighbouring chromophores are described using a Frenkel exciton model [12, 14]. The model features two excitonic absorption bands for each tubule (inner and outer) of the aggregate. The two bands are caused by transitions polarized parallel and perpendicular to the aggregate's main axis. The different diameters of the inner and outer tubules lead to a slightly different arrangement of C8S3 chromophores. Since the energies of optical transitions are highly sensitive to the microscopic structure of cylindrical aggregates, the spectral positions of the absorption bands are different [12]. This allows for the selective optical study of each tubule. Exciton dynamics in multiple double-wall cylinders twisted into helices (C8O3 aggregates) were extensively studied at room temperature. The studies revealed a weak coupling between the inner and outer walls of the aggregate and ultrafast (on a sub-picosecond timescale) outer-to-inner tubule excitonic energy transfer (ET) [15-17 and chapters 2 and 3 of this thesis]. In this chapter we examine exciton dynamics in C8S3 aggregates at cryogenic temperature by means of femtosecond frequency-resolved pump-probe spectroscopy. The studies were inspired by time-resolved fluorescence measurements at low temperatures which disclosed a complicated optical behaviour based on inter tubule ET and restrained excitonic energy relaxation within the excitonic manifolds of the aggregate [18 and chapter 4]. However, the time resolution of the fluorescence measurements was limited to 8 ps, which obscured observation of fast initial processes.
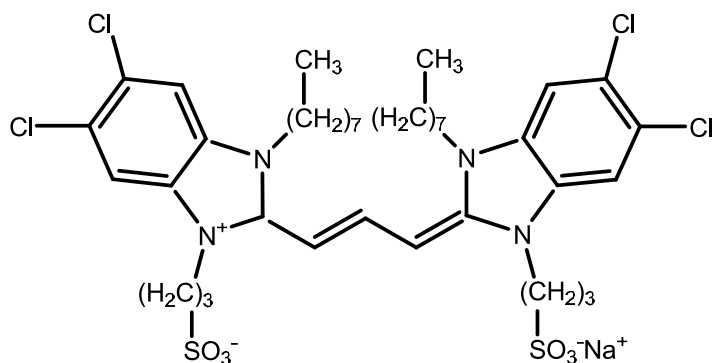

Figure 1. Chemical structure of C8S3 chromophore.

II. EXPERIMENT

The C8S3 dyes were purchased from FEW Chemical and used without further purification. 6.2×10^{-3} M solutions were prepared by dissolving the dye in MilliQ-grade water and stirring at room temperature for at least 24 hours for aggregation to take place. A droplet of the aggregate solution was squeezed between 0.12-mm microscope cover slips, rapidly cooled to 77 K in liquid nitrogen and transferred into a He continuous-flow cryostat (CF1204SEG, Oxford Instruments). Details on experimental facilities and frequency-resolved pump-probe experiments are given elsewhere [16]. The excitation wavelength was 585 nm to selectively excite the outer tubule, while the spectrum of the probe light covered the spectral range of 570-630 nm, sufficient for simultaneous observation of the response from both

tubules. The excitation density was attenuated to about 1 photon absorbed per 2000 chromophores to prevent exciton-exciton annihilation. Experiments were performed at a temperature of 7 K.

III. Results and Discussion

The measured pump-probe spectra (see Fig. 2) exhibit the dispersive shape typical for J-aggregates, with photoinduced absorption blue shifted with respect to the bleaching – stimulated emission bands. The two pairs of photoinduced absorption and bleaching – stimulated emission bands correspond to the linear absorption bands **1** and **2** centred at 596 nm and 586 nm characteristic for the inner and outer tubules respectively [12]. The measured pump-probe spectra agree qualitatively with the ones modelled theoretically for cylindrical aggregates [19]. As one can see from Fig. 2 and 3, after the excitation at 585 nm, the signal in the vicinity of band **2** decays rapidly, while the signal in the vicinity of band **1** features delayed formation on a timescale of a few picoseconds. Note that the instantaneously induced pump-probe signal around 596 nm is caused by the limited spectral selectivity of the excitation. The precursor-successor relation clearly seen in Fig. 3 evidences the presence of outer-to-inner tubule ET.
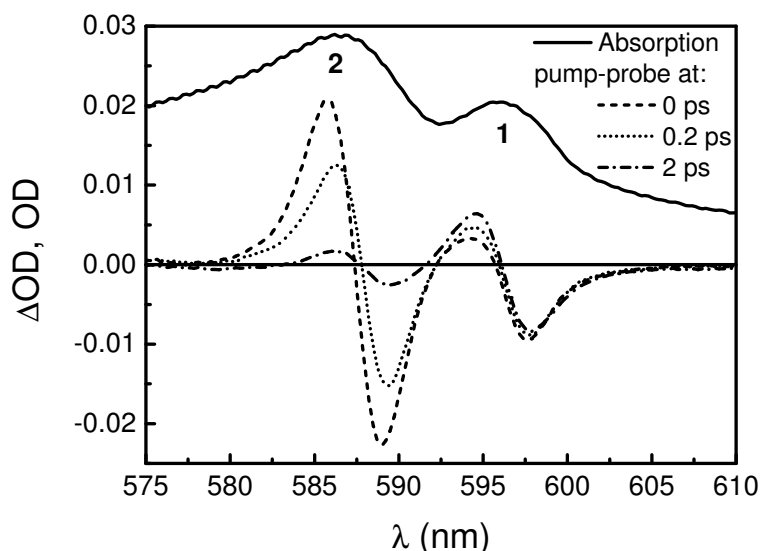

Figure 2. Absorption spectrum of C8S3 aggregates at 7 K (only the two lowest energy bands, scaled down by a factor of 30) and pump-probe dynamics during the first 2 ps after the excitation at 585 nm.

The dynamics of the pump-probe spectra were characterized by analyzing the pump-probe transients at different probe wavelengths corresponding to different transitions. In view of the fact that all the bands of the pump-probe spectra largely overlap and influence the amplitude and positions of each other, the data was deconvoluted prior to further analysis. To deconvolute the data, the relative contributions of the bands to the amplitudes of their neighbours were estimated and a set of linear equations was solved to extract undistorted band peak amplitudes. The pump-probe signal in the vicinity of band **2** (Fig. 4) decays two exponentially with decay time constants of (334 ± 50) fs and (21 ± 5) ps. The 21 ps decay time constant agrees with the fluorescence lifetime of C8S3 aggregates reported earlier [18 and chapter 4]. As one can see from the Fig. 4, the formation of the signal in the vicinity of band **1**, however, is substantially slower than the decay of the signal in the vicinity of band **2**.

The different decay and delayed formation rates for the bands **1** and **2** (334 fs and about 2 ps, respectively) strongly suggest that intermediate states are involved in the ET process. These intermediate states are not observed in the transient spectra because they are optically inactive. As it was recently demonstrated for two closely spaced linear aggregates, the excitation ET may occur from or toward a low transition dipole moment (optically dark) exciton state, implying that overlap of optical spectra is not a requirement for ET [20]. Since a double-wall tubular aggregate is qualitatively equivalent to a system of two closely spaced linear aggregates, similar ET pathways can be considered. First, the excitation energy from the outer tubule is transferred to the higher-lying optically inactive states of the excitonic manifold of the inner tubule. Second, the intra-band relaxation takes place and excitations reach the low lying optically active energy states which contribute to the pump-probe signal.
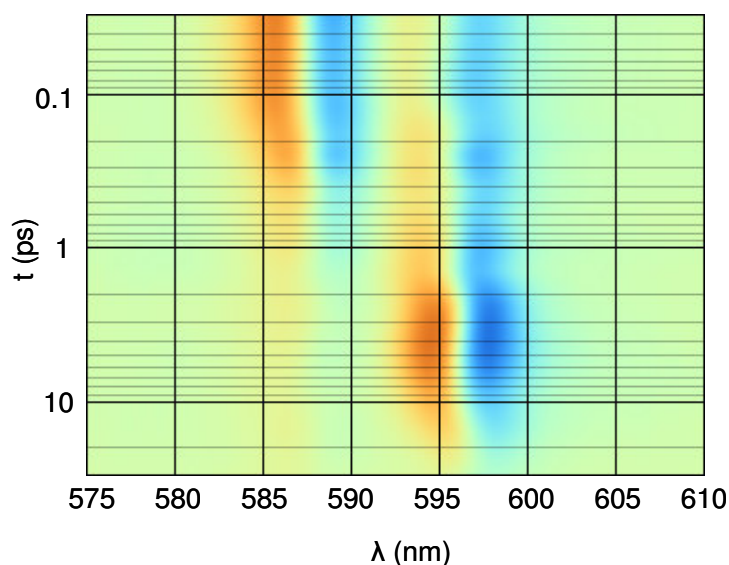

Figure 3. Chrono-spectroscopic dynamics of the pump-probe signal after the excitation at 585 nm. Red regions show photoinduced absorption; blue regions show bleaching and stimulated emission.
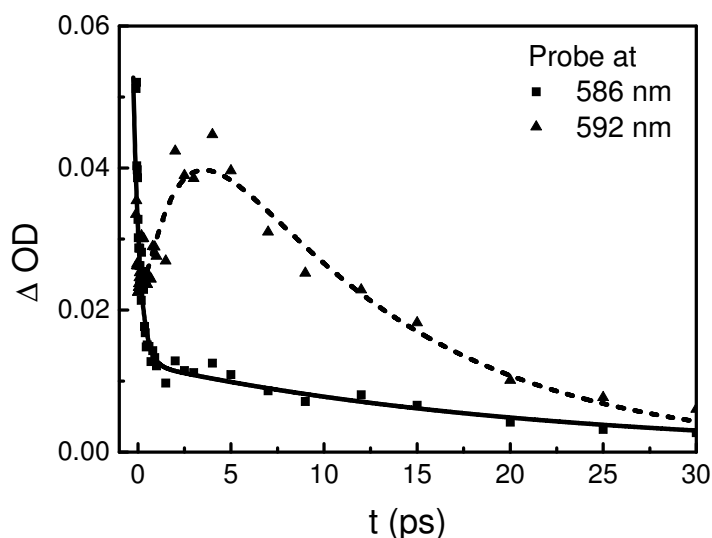

Figure 4. Dynamics of the pump-probe signal amplitudes for the 586 nm and 596 nm bands. The solid curve represents a two exponential fit for the signal of band **2**, the dashed curve – a three exponential fit for the signal of band **1**.

On the basis of such two-step ET model, in order to characterize the dynamics in the vicinity of band **1**, the data were fitted with three exponents. The first time constant was fixed to 334 fs, the fitting revealed two additional time constants: (2 ± 0.7) ps for formation and (11 ± 2) ps for decay. Although the error bars on the time constants are significant, they differ from each other by nearly an order of magnitude. This allows for a straightforward assignment of the time constants to different relaxation steps with an adequate accuracy. In particular, the obtained time constant of (2 ± 0.7) ps is characteristic for the intra-band relaxation from optically inactive to optically active energy states. Because of its rather fast relaxation, the process was not observed in time-resolved fluorescence experiments in the previous chapter (see also Ref. [18]).
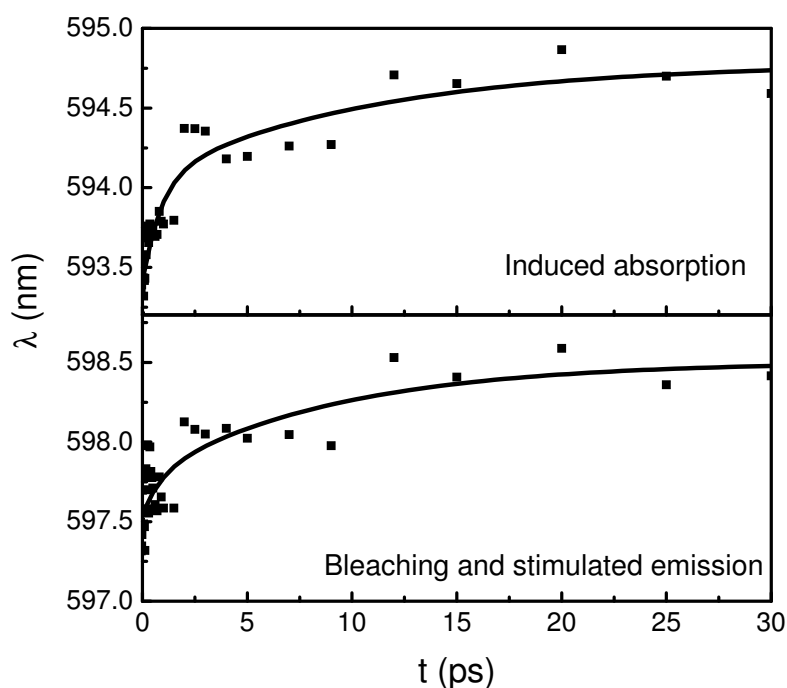

Figure 5. Spectral dynamics of the inner tubule pump-probe signal. Peak positions of induced absorption and bleaching – stimulated emission bands are displayed as squares; two exponential fits, as solid curves.

Apart from the ET related decay and delayed formation of the signal in the vicinity of bands **2** and **1** respectively, a dynamic Stokes-shift for all induced absorption and bleaching – stimulated emission bands is observed (Fig. 2, 3). The time-dependent maxima positions of the photoinduced absorption and bleaching – stimulated emission bands corresponding to the exciton located on the inner wall are shown in Fig. 5. The dynamics of the spectral shifts are characterized by time constants of 900 fs and 10 ps, which, in analogy with the analysis of pump-probe transients discussed above and time-resolved fluorescence data, can be attributed to initial fast population of optically active states and to substantially slower intra-band relaxation in between optically active states respectively. As discussed in chapter 4 and in Ref. [18], the substantially slower intra-band relaxation between the optically active states is caused by a disorder induced localization of the excitonic wavefunctions, which tend to be most pronounced in the lowest energy states of the excitonic manifold.

IV. CONCLUSIONS

Exciton dynamics in the double-wall cylindrical aggregates of the C8S3 cyanine dye have been examined by means of femtosecond pump-probe spectroscopy at cryogenic temperature. Both inter-tubule ET and intra-tubule energy relaxation were observed. On the basis of the experimental evidence, a two-step outer-to-inner tubule ET model is proposed. First, the excitation energy from the outer tubule is transferred to the dark states of the inner tubule with a time constant of (334 ± 50) fs. Second, relaxation to the optically active states within the excitonic manifold of the inner cylinder takes place with a time constant of (2 ± 0.7) ps. In addition, spectral dynamics on a picosecond timescale is observed. This spectral dynamics is attributed to the energy relaxation between optically active states in the excitonic manifold, in accordance with the time-resolved fluorescence observations. The measured intra-band relaxation rate from the dark to the optically active states supplements the work presented previously [18 and chapter 4] and comprehensively contributes to the general understanding of ET dynamics in double-wall cylindrical aggregates.

REFERENCES

1. E. E. Jelley, *Nature* **138**, 1009 (1936).
2. G. Scheibe, *Angew. Chem.* **49**, 563 (1936).
3. T. Kobayashi, *J-Aggregates* (World Scientific, Singapore, 1996).
4. J. Knoester, in: *Organic Nanostructures: Science and Application*, edited by V. M. Agranovich, G. C. La Rocca, p. 149 (IOS Press, Amsterdam, 2002).
5. A. Mishra, R. K. Behera, P. K. Behera, B. K. Mishra, G. B. Behera, *Chem. Rev.* **100**, 1973 (2000).
6. F. Wurtner, R. Wortmann, K. Meerholtz, *Chem. Phys. Chem.* **3**, 117 (2002).
7. V. I. Prokhorenko, A. R. Holzwarth, M. G. Muller, K. Schaffner, T. Miyatake, H. Tamiaki, *J. Phys. Chem. B* **106**, 5761 (2002).
8. H. van Amerongen, L. Valkunas, R. van Grondelle, *Photosynthetic Excitons* (World Scientific, Singapore, 2000).
9. G. McDermot, S. M. Prince, A. A. Freer, A. M. Hawthornthwaite-Lawless, M. Z. Papiz, R. J. Cogdell, N. W. Isaac, *Nature* **374**, 517 (1995).
10. S. C. Doan, S. Shanmugham, D. E. Aston, J. L. McHale, *J. Am. Chem. Soc.* **127**, 5885 (2005).
11. R. Rotomskis, R. Augulis, V. Snitka, R. Valiokas, B. Liedberg, *J. Phys. Chem. B* **108**, 2833 (2004).
12. C. Didraga, A. Pugžlys, P. R. Hania, H. von Berlepsch, K. Duppen, J. Knoester, *J. Phys. Chem. B* **108**, 14976 (2004).
13. H. von Berlepsch, C. Böttcher, A. Ouart, M. Regenbrecht, S. Akari, U. Keiderling, H. Schnablegger, S. Dähne, S. Kirstein, *Langmuir* **16**, 5908 (2000).
14. C. Didraga, J. Klugkist, J. Knoester, *J. Phys. Chem. B* **106**, 11474 (2002).
15. A. Pugžlys, P. R. Hania, C. Didraga, V. A. Malyshev, J. Knoester, K. Duppen, *Springer Series in Chemical Physics* **79**, 879 (2004).
16. A. Pugžlys, P. R. Hania, C. Didraga, J. Knoester, K. Duppen, *Solid State Phenomena* **97-98**, 201 (2004).
17. A. Pugžlys, P. R. Hania, R. Augulis, K. Duppen, P. H. M. van Loosdrecht, *Int. J. Photoenergy*, 29623 (2006).
18. A. Pugžlys, R. Augulis, P. H. M. van Loosdrecht, C. Didraga, V. A. Malyshev, J. Knoester, *J. Phys. Chem. B* **110**, 20268 (2006).

19. M. Bednraz, J. Knoester, *J. Phys. Chem. B* **105**, 12913 (2001).
20. C. Didraga, V. A. Malyshev, J. Knoester, *J. Phys. Chem. B* **110**, 18818 (2006).